

U S-F T /30-95

$F_2/xG(x, Q^2)$ RATIO AT SMALL x AND THE ROLE OF THE
CONTRIBUTION FROM INFRARED REGION

M G Ryskin and A G Shuvaev

Petersburg Nuclear Physics Institute,
Gatchina, St.Petersburg 188350 Russia

and

Yu M Shabelski

Departamento de Física de Partículas,
Universidad de Santiago de Compostela,
15706 Santiago de Compostela, Spain

Abstract

We consider the light quark electroproduction cross section and show that the contribution coming from the infrared ($q_T < 300 \text{ MeV}$) region is not negligible. It changes the $F_2(x; Q^2) = xG(x; Q^2)$ ratio by 20-30% (or even more) for small x and $Q^2 \sim 4 \text{ GeV}^2$.

E-mail RYSKIN@THD.PNPI.SPB.RU

E-mail SHABELSKI@THD.PNPI.SPB.RU

E-mail SHUVAEV@THD.PNPI.SPB.RU

*) Permanent address: Petersburg Nuclear Physics Institute,
Gatchina, Saint-Petersburg 188350, Russia.

December 1995

U S-F T /30-95

1 INTRODUCTION

In the present paper we will consider the relation between the deep inelastic structure function $F_2(x; Q^2)$ and the gluon density $xG(x; Q^2)$ in the region of small x . At very small x the main contribution to F_2 comes from the sea quarks and the value of DIS cross section is given by the photon-gluon fusion subprocess Fig. 1. For large Q^2 in the Leading Log Q^2 Approximation (LL_QA) and in a physical (say, axial) gauge it is enough to deal only with the diagram Fig. 1a. However within the LLog($\frac{1}{x}$)A, which sums up all the terms of the type $(\ln \frac{1}{x})^n$, one has to take into account the graph Fig. 1b also.

Based on these graphs Fig. 1 one can extract the value of the gluon structure function $G(x; k^2)$ from the experiment, where the DIS structure function $F_2(x; Q^2)$ was measured.

The question we are going to discuss here in more detail is: what are the values of gluon kinematical variables x_g and k^2 which correspond to the arguments $x = x_B$ and Q^2 of the DIS cross section; i.e. F_2 ?

In Sect. 2 we will remind the LL_xA formulae [1] for the function F_2 (and F_L) written in the framework of the high energy k_t -factorization scheme [2], where the gluon k (see Fig. 1) is on mass-shell.

Then by the numerical computation in Sect. 3 we will study the ratios of the deep inelastic (Bjorken) variables (x_B and Q^2) and the values of the gluon's momenta (x_g and k^2 correspondingly), which are essential in the integrals of Eqs. (3) and (13); and how do these ratios depend on the form of the gluon structure function.

To answer the last question we parametrize the gluon density by the power functions $xG(x; k^2) = x \cdot \frac{1}{k^2} \cdot \frac{1}{x}$ and plot the logarithms of the ratios $(\ln \frac{x_g}{x_B}; \ln \frac{k^2}{Q^2}; \ln \frac{Q^2}{Q_0^2})$ as the functions of powers α and β .

Even in the case of a strong scaling violation ($\alpha = \frac{1}{2}$) the average value $\langle \ln \frac{Q^2}{k^2} \rangle$ turns out to be rather large. It corresponds to $k^2 = 0.8 - 2 \text{ GeV}^2$ for $Q^2 = 16 - 64 \text{ GeV}^2$.

Thus there appears a danger that an important part of $F_2(x; Q^2)$ is originated from the region of a small gluon's transverse momentum (virtualities) ($k_t < 1 \text{ GeV}$), where the perturbative QCD approach is not justified.

To follow the role of the infrared (small q_t) region we have changed also the mass of a light quark¹. The value of F_2 increases up to the factor of 1.5 - 2 when instead of the constituent mass $m_q = 350 \text{ MeV}$ one puts the small (close to the current) mass $m_q = 10 \text{ MeV}$. The situation becomes slightly better if we assume the saturation of gluon distributions at small x and k^2 .

¹The heavy quark contribution to F_2 was discussed in the previous paper [1].

At very small x and k^2 the cross section $\frac{xG(x;k^2)}{k^2}$ should tend to a constant. Thus at $k^2 < k_0^2$ (for example we put here $k_0^2 = 1 \text{ GeV}^2$) the gluon density $xG(x;k^2) \sim k^2$; in other words at $k^2 \sim 1 \text{ GeV}^2$ the anomalous dimension $\gamma = 1$. In this case the rapid decrease of $G(x;k^2)$ at $k^2 \rightarrow 0$ suppresses the role of the infrared region and the result becomes more stable (under the variation of m_q). This point will be discussed also in Sect. 3.

Finally we have to stress that the infrared ($q_t; k_t < 0.4 \text{ GeV}$) region gives not too small contribution to the $\frac{F_2(x;Q^2)}{xG(x;Q^2)}$ ratio and one has to remember about it, trying to extract the gluon structure function from the $F_2(x;Q^2)$ experimental data.

2 SMALL x DIS CROSS SECTIONS

The cross section of heavy quarks as well as light quarks (if Q^2 value is large enough) electroproduction is given schematically by the graphs in Fig. 1. The main contribution to the cross section at small x is known to come from gluons. The lower ladder blocks presents the two-dimensional gluon distribution $'(x;k^2)$ which is a function of the fraction x of the longitudinal momentum of the initial hadron and the gluon virtuality. Its distribution over x and transverse momenta k_T in hadron is given in the semi-hard theory [3] by function $'(x;k^2)$. It differs from the usual gluon structure function $G(x;q^2)$:

$$xG(x;q^2) = \frac{1}{4} \frac{1}{2} \int_0^{q^2} '(x;q_1^2) dq_1^2 : \quad (1)$$

Such definition of $'(x;k^2)$ makes possible to treat correctly the effects arising from gluons virtualities. The exact expression for this function can be obtained as a solution of the evolution equation which, contrary to the parton model case, is nonlinear due to interactions between the partons in small x region.

In what follows we use Sudakov decomposition for the produced quarks' momenta $p_{1,2}$ through the light-like momenta of colliding particles $p_A \sim Q$ and p_B ($p_A^2 = p_B^2 = 0$) and transverse ones $p_{1,2T}$:

$$p_{1,2} = x_{1,2} p_B + y_{1,2} p_A + p_{1,2T} : \quad (2)$$

The differential cross sections of a quark pair electroproduction² have the

² $\sigma_{e,p;L}$ denotes the virtual photon-proton transverse and longitudinal cross sections.

form³:

$$\frac{d_{\text{el},T,L}}{dy_1 dy_2 d^2 p_{1T} d^2 p_{2T}} = \frac{e_{\text{em}}^2}{(2)^4} \frac{1}{(s)^2} \int d^2 k_T (k_T - p_T - p_T) (y_1 + y_2 - 1) \frac{s(k^2)}{k^2}, \quad (k^2; x) M_{\text{el},T,L}^2 \frac{1}{Y_2} : \quad (3)$$

Here $s = 2p_A p_B$, k is the gluon transverse momentum and y is the quarks rapidity in the $^?$ p c.m.s. frames,

$$x_1 = \frac{p_{1T}}{p_s} e^{y_1}; \quad x_2 = \frac{p_{2T}}{p_s} e^{y_2}; \quad x = x_1 + x_2; \\ y_1 = \frac{p_{1T}}{p_s} e^{y_1}; \quad y_2 = \frac{p_{2T}}{p_s} e^{y_2}; \quad m_T = \sqrt{p_T^2 + m^2} : \quad (4)$$

$M_{\text{el},T,L}^2$ are the squares of the matrix elements [1] for the cases of transverse and longitudinal electroproduction, respectively.

In LLA kinematic

$$k' = x p_B + k_T ; \quad (5)$$

so

$$k^2 = k_T^2 : \quad (6)$$

(The more accurate relation is $k^2 = \frac{k_T^2}{1-x}$ but we are working in the kinematics where $x; y \rightarrow 0$).

The matrix elements M are calculated in the Born order of QCD without standart simplifications of the parton model since in the small x domain there are no grounds for neglecting the transverse momenta of the gluon k_T in comparison with the quark masses and transverse momenta, especially in the case of light quark pair production. In the axial gauge $p_B A = 0$ the gluon propagator takes the form $D(k) = d(k) = k^2$;

$$d(k) = (k p_B + k p_B) = (p_B k) : \quad (7)$$

For the gluons in t-channel the main contribution comes from the so called 'nonsense' polarization g^n , which can be picked out by decomposing the numerator into longitudinal and transverse parts:

$$(k) = 2(p_B p_A + p_A p_B) = s + \dots \quad 2p_B p_A = s \quad g^n : \quad (8)$$

The other contributions are suppressed by the powers of s . Since the sum of the diagrams in Fig. 1 are gauge invariant in the LLA, the transversality

³We put the argument of s to be equal to gluon virtuality, which is very close to the BLM scheme [4]; (see also [5]).

condition for the ends of gluon line enables one to replace p_A by $k_{1T}=x$ in expression for g^n . Thus we get

$$d(k) = \frac{p_B k_T}{2 x s} \quad (9)$$

or

$$d(k) = \frac{k_T k_T}{2 x y s} \quad (10)$$

if we do such a trick for vector p_B too. Both these equations for d can be used but for the form (9) one has to modify the gluon vertex slightly (to account for several ways of gluon emission { see Ref. [5] }):

$$d_{eff} = \frac{2}{xys} [(xys - k_{1T}^2) k_{1T} - k_{1T}^2 k_{2T} + 2x (k_{1T} k_{2T}) p_B]: \quad (11)$$

As a result the colliding gluons can be treated as aligned ones and their polarization vectors are directed along the transverse momenta. Ultimately, the nontrivial azimuthal correlations must arise between the transverse momenta p_{1T} and p_{2T} of the produced quarks.

In the case of photoproduction the alignment of the gluon makes the distribution of the difference of the transverse momenta of the quarks $p_T = (p_1 - p_2)_T = 2$ to be proportional to $1 + \cos^2 \theta$, where θ is the angle between the vectors p_T and $k_T = (p_1 + p_2)_T = 2$.

Although the situation considered here seems to be quite opposite to the parton model there is a certain limit in which our formulae can be transformed into parton model ones. Let us consider the case of pp collisions and assume now that the characteristic values of quarks' momenta p_{1T} and p_{2T} are many times larger than the values of gluons' momenta, k_{1T} and k_{2T}

$$\langle p_{1T} \rangle \gg \langle k_{1T} \rangle; \langle p_{2T} \rangle \gg \langle k_{2T} \rangle; \quad (12)$$

and one can keep only lowest powers of $k_{1T}; k_{2T}$. It means that we can put $k_{1T} = k_{2T} = 0$ everywhere in the matrix element M except the vertices, as it was done in the parton model approach.

On the other hand, the used assumption (12) is not fulfilled in a more or less realistic case. The transverse momenta of produced light quarks should be of the order of gluon virtualities (QCD scale values).

3 RESULTS OF CALCULATIONS AND DISCUSSION

The function $'(y; k^2)$ is unknown at small values of k^2 . Therefore we rewrite the integrals over k_2 in Eq. (3) in the form

$$\begin{aligned} & \int_0^{Z_1} dk_T^2 (k_T^2, p_T^2, p_T^2) (y_1 + y_2 - 1) \frac{s(k^2)}{k^2} ' (k^2; x) \int \frac{1}{Y_2} = \\ & \frac{P}{4} \frac{1}{2} \int_0^{Z_1} dk_T^2 (k_T^2, p_T^2, p_T^2) (y_1 + y_2 - 1) s(Q_0^2) x G(x; Q_0^2) \frac{1}{k^2} \int \frac{1}{Y_2} \quad (13) \\ & + \int_{Q_0^2}^{Z_1} dk_T^2 (k_T^2, p_T^2, p_T^2) (y_1 + y_2 - 1) \frac{s(k^2)}{k^2} ' (k^2; x) \int \frac{1}{Y_2} ; \end{aligned}$$

where Eq. (1) is used.

Using Eq. (3) and Eq. (13) we perform the numerical calculation of light quark production.

The results of computations are presented in Figs. 2-8. In Figs. 2 and 3 we plot the values of $F_2(x; Q^2)$ coming from the sea $u + \bar{u}$ quark contribution in the cases of MT (S-DIS) [6] and GRV HO [7] gluon distributions, respectively. The parameter Q_0 in Eq. (13) which separates the region of 'small' and 'large' gluon momenta k_t was chosen to be equal to 1 GeV (Figs. 2a and 3a) and 2 GeV (Figs. 2b and 3b). It is seen that the results depend rather strongly on the value of Q_0 as well as on the mass of light quark and in both cases are differed from the original MT (S-DIS) (or GRV HO) predictions for $u + \bar{u}$ sea quark contribution (which, in our notations correspond to $Q_0^2 > Q^2$ and $m_q = 0$) and shown by solid curves in Figs. 2 and 3. However the difference of our calculated $F_2(x; Q^2)$ values and the original ones is not large. It means that both the procedure of the gluon density extraction from $F_2(x; Q^2)$ experimental data and the accuracy of our calculations are reasonably enough and there is no a large contribution of any (say, nonperturbative) corrections.

The only explanation is the contribution of the small transverse momenta $k_t \leq Q_0$ and $q_t \leq m_q$ to the final value of F_2 . Even for $Q^2 = 64 \text{ GeV}^2$ the difference between the cases of $m_q = 10 \text{ MeV}$ and 100 MeV is of about 20% (up to 30% for GRV HO and $Q_0 = 1 \text{ GeV}$) at $x = 10^{-3}$.

To understand better what are the typical quark (q_t) and gluon ($k_t; x_g$) momenta, which are essential in the integrals Eq. (13), we have chose the parametrization of gluon distribution in the form

$$xG(x; Q^2) = 15 \frac{x}{0.001} \frac{Q^2}{20 \text{ GeV}^2} \quad (14)$$

and calculated the mean values of logarithms $r_q = \langle \ln \frac{q^2}{Q^2} \rangle$, $r_k = \langle \ln \frac{k_t^2}{Q^2} \rangle$ and $r_x = \langle \ln \frac{x_B}{x_q} \rangle$.

The advantage of the logarithms is that they do not destroy the main power structure of the integrand (trying to estimate directly the value of $\langle k^2 \rangle$ or $\langle \frac{1}{k^2} \rangle$, one faces the divergence of the integral over dk^2 at large (small) k_t^2 for the positive $\beta < 1$).

The ratio of the sea u-quark to the gluon densities are given in Fig. 4 (in terms of $F_2(x; Q^2)$ and $xG(x; Q^2)$ structure functions) for different values of β (0.2 and 0.5) and α (0.2 and 0.5) in Eq. (14). At very small $x < 3 \cdot 10^{-3}$ this ratio tends to a constant and does not depend on x . However, even at large $\beta = 1/2$ (the value which corresponds to the asymptotics (extremum) of the BFKL solution) when from the formal point of view the convergence of the integral in the infrared region should be good enough, the dependence of the result on the light quark mass is still not negligible (20% difference between the values of F_2 for $m_q = 350$ MeV and 10 MeV at $x = 10^{-3}$ and $Q^2 = 16$ GeV²).

The situation becomes slightly better (see Fig. 5) if one assumes that for small Q^2 the gluon density falls down as $xG(x; Q^2) \sim Q^2$ (say, $\beta = 1$ for $Q^2 < 1$ GeV²). Such a behaviour one might expect in the case of the gluon density saturation [3] (i.e. $(Q^2)^{-\frac{xG(x; Q^2)}{Q^2}} \rightarrow \text{const at } Q^2 \rightarrow 0$).

Unfortunately, the saturation hypothesis is also not enough to neglect completely the small q_t contribution. Increasing the quark mass from 10 MeV to 350 MeV one diminishes the cross section more than 15% (for example, at $x = 10^{-3}$; $Q^2 = 16$ GeV², $\beta = 0.5$; and 20% for $\beta = 0.5$, without the saturation).

This fact is confirmed by the β -dependence of the function r_k (Fig. 7a). As it should be expected the value of r_k depends slowly on β but noticeably increases with β . For a more heavy photon ($Q^2 = 64$ GeV²) r_k becomes smaller. It means that the typical values of k_t^2 increases with Q^2 not as quickly as Q^2 (more close to $\sqrt{Q^2}$). In the best case ($\beta = 0.5$ for $Q^2 > 1$ GeV² and $\beta = 1$ for $Q^2 < 1$ GeV²) the value of r_k (≈ 1.7 at $Q^2 = 16$ GeV²) corresponds to k_t^2 , essential in the integral, of about 3 GeV² (smaller than the usual cut $Q_0^2 = 4 \div 5$ GeV² for the MT or MSR parametrizations [6, 8] of the structure functions). Without the saturation at $Q^2 = 16$ GeV² the $r_k \approx 3$; i.e. typical $k_t \approx 0.8$ GeV.

In order to estimate the values of the longitudinal gluon momenta (x_g) we plot in Fig. 8 the logarithms of the x_B to x_g ratios. The last ratios increase with Q^2 as for a small Q^2 the transverse momenta of quarks sometimes becomes larger than the photon virtuality ($\sqrt{Q^2}$), see Fig. 6, and one needs a large x_g of gluon to put these quarks on mass shell. In the region of $Q^2 = 16$ GeV² the value $r_x \approx 1.2$; it means that as an average the gluon x_g is 3

times larger than the Bjorken x_B . This result slightly differs from the Prytz estimation [9] where a gluon has $x_g = 2x_B$.

The value of $F_2(x; Q^2)$ is the sum of transverse (F_{2T}) and longitudinal (F_{2L}) contributions. As one can see from the Table, at large Q^2 the last contribution is more infrared stable.

4 CONCLUSION

We hope that the ratio of F_2 to $xG(x; Q^2)$ presented in Figs. 4, 5 as a functions of anomalous dimension and intercept may be used in future in order to extract, for example, the values of gluon density directly from the F_2 structure function (in this case the values of γ and α are also come from the F_2 data as $\gamma = d \ln F_2 / d \ln Q^2$ and $\alpha = d \ln F_2 / d \ln(1/x)$).

The results we have presented here are close to the standard gluon densities extracted from the derivative $dF_2(x; Q^2) = d \ln(Q^2)$ (using the Prytz method [9], or the modified one, taken into account the NLO corrections [10]). Nevertheless, here we better understand the typical values of gluon momenta we deal with and can control the role of the small k_T (infrared) region.

The mean logarithms $r_q; r_k$ and r_x give us an estimate of the quark transverse momenta which are essential in the process, and the values of gluon virtuality (k^2) and proton momentum fraction (x_g) which correspond to the point x_B and Q^2 for the structure function F_2 .

A lesson one has to extract from these calculations is the fact that an essential values of transverse momenta (q_t) which do contribute to the next-to-leading order (NLO) corrections may be quite differ from the initial Q^2 . At not too large Q^2 the value of q_t^2 may be even larger than Q^2 (in Fig. 6 $r_q > 0$ for $Q^2 = 16 \text{ GeV}^2$).

However the main danger comes from the cases where the virtuality in the internal loops is much smaller than Q^2 . For example when (as it was done in [11]) one includes in the anomalous dimension (!) the NLO corrections of the type $(\gamma_s = !)^n$ in the first non-zero (4-loops) gluon-gluon correction $(\gamma_s = !)^4$, he touches the region of the internal $q^2 \ll Q^2$; down to $q^2 \ll Q^2 = 100$ due to the large numerical coefficient $\beta_0 = 14/3$ in the Lipatov [12] diffusion-like distribution $\exp[-\ln(q^2/Q^2) = (4/\gamma)] = \exp[-\ln(q^2/Q^2) = (a/n)]$ where $a = -\ln 2 \approx 0.7$ and n is the number of loops. After this we use the value of the anomalous dimension (!) (including the NLO corrections) as a local (from the point of view of $\ln Q^2$ space) contribution at the given point Q^2 .

There are no problems if Q^2 is very large but one can not to do this for not too large Q^2 where the essential transverse momenta of intermediate gluons

may be rather small; close to the infrared region ($Q=10 \Lambda_{\text{QCD}}$).

This work is supported by the Grant INTAS-93-0079.

Table 1

Transverse and longitudinal contributions to $F_2(x; Q^2)$ for $u\bar{u}$ pair production at several points.

	x	$m_q, M \text{ eV}$	$Q^2 = 4 \text{ GeV}^2$		$Q^2 = 64 \text{ GeV}^2$	
			F_{2T}	F_{2L}	F_{2T}	F_{2L}
Without saturation	0.0016	10	0.126	0.0354	.392	0.105
		350	0.0816	0.0242	.346	0.102
	0.0064	10	0.0593	0.0170	0.186	0.505
		350	0.0378	0.0116	0.163	0.489
With saturation	0.0016	10	0.102	0.331	0.369	0.104
		350	0.0763	0.0230	0.338	0.101
	0.0064	10	0.0479	0.0159	0.175	0.0500
		350	0.0352	0.0110	0.159	0.0484

Figure captions

Fig. 1. Low order QCD diagrams for quark pair electroproduction via photon-gluon fusion.

Fig. 2. $u + \bar{u}$ sea quark contributions to $F_2(x; Q^2)$ as given by M T S-D IS [6] sea quark distributions (solid curves) and our calculations using M T S-D IS gluon distributions for $m_q = 10 \text{ MeV}$ and 100 MeV (dashed and dash-dotted curves, respectively). The values of Q_0 parameter equal to 1 GeV (a) and 2 GeV (b) were used in Eq. (13)

Fig. 3. The same as Fig. 2 but for GRV HO [7] parton distribution.

Fig. 4. The ratios $F_2(x; Q^2)$ ($u + \bar{u}$ sea quark contribution) to $xG(x; Q^2)$ calculated from Eqs. (13), (14) for different values α_s and β_1 .

Fig. 5. The same as Fig. 4 assuming that at $Q^2 < 1 \text{ GeV}^2$ $\alpha_s = 1$ (i.e. saturation effect).

Fig. 6. $r_q = \langle \ln \frac{q_q^2}{Q^2} \rangle$ dependences on α_s (a) and β_1 (b).

Fig. 7. $r_k = \langle \ln \frac{k_q^2}{Q^2} \rangle$ dependences on α_s (a) and β_1 (b).

Fig. 8. $r_x = \langle \ln \frac{x_B}{x_q} \rangle$ dependences on α_s (a) and β_1 (b).

References

- [1] Ryskin M.G., Shabelski Yu.M., Shuvaev A.G. : Z Phys C (in print); preprint Santiago Univ. US-FT/11-95; hep-ph/9506338.
- [2] Catani S., Ciafaloni M. and Hautmann F. : Phys.Lett. B 242 (1990) 97; NuclPhys. B 366 (1991) 135; Phys.Lett B 307 (1993) 147.
- [3] Gribov L.V., Levin E.M. and Ryskin M.G. : PhysRep., 1983, v.100, p.1; Levin E.M. and Ryskin M.G. : PhysRep., 1990, v.189, p.267.
- [4] Brodsky S.J., Lepage G.P. and Mackenzie P.B. : Phys. Rev., 1983, v.D 28, p.228.
- [5] Levin E.M., Ryskin M.G., Shabelski Yu.M., Shuvaev A.G. : Yad.Fiz. 1991, v.54, p.1420.
- [6] Morin J.G. and Tung W.-K. : Z Phys. 1991, v.C 52, p.13.
- [7] Gluck M., Reya E. and Vogt A. : Z Phys. 1993, v.C 53, p.127.
- [8] Martin A.D., Stirling W.J. and Roberts R.G. : Preprint RAL 94-055, DTP/94/34 (1994).
- [9] Prytz K. : Phys.Lett. 1993, v.B 311, p.286.
- [10] Prytz K. : Phys.Lett. 1994, v.B 332, p.393.
- [11] Ellis R.K., Hautmann F. and Webber B.R. : Preprint FNAL-PUB-95/006-T (1995), Cavendish-HEP-94/18; Ellis R.K., Kunszt Z. and Levin E.M. : NuclPhys., 1994, v.B 420, p.517; Catani S. and Hautmann F. : NuclPhys. B 427 (1994) 475.
- [12] Lipatov L.N. : Sov.J.JETP 1986, v.90, p.1536.

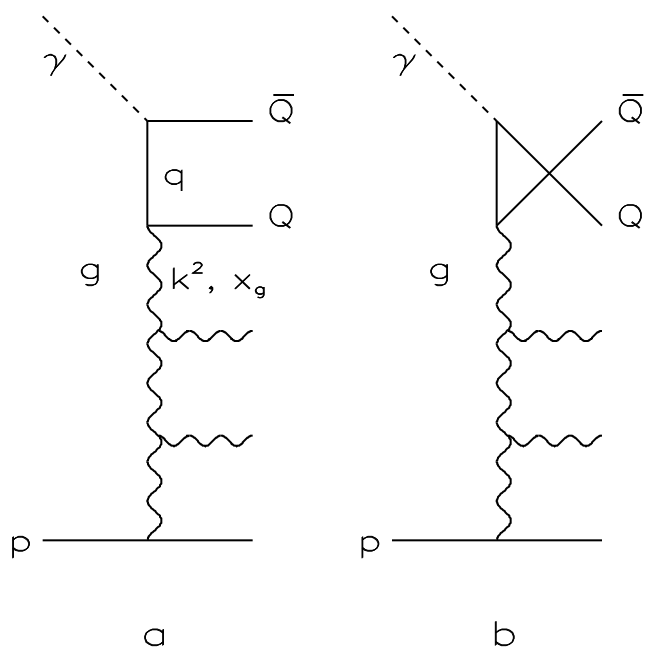


Fig. 1

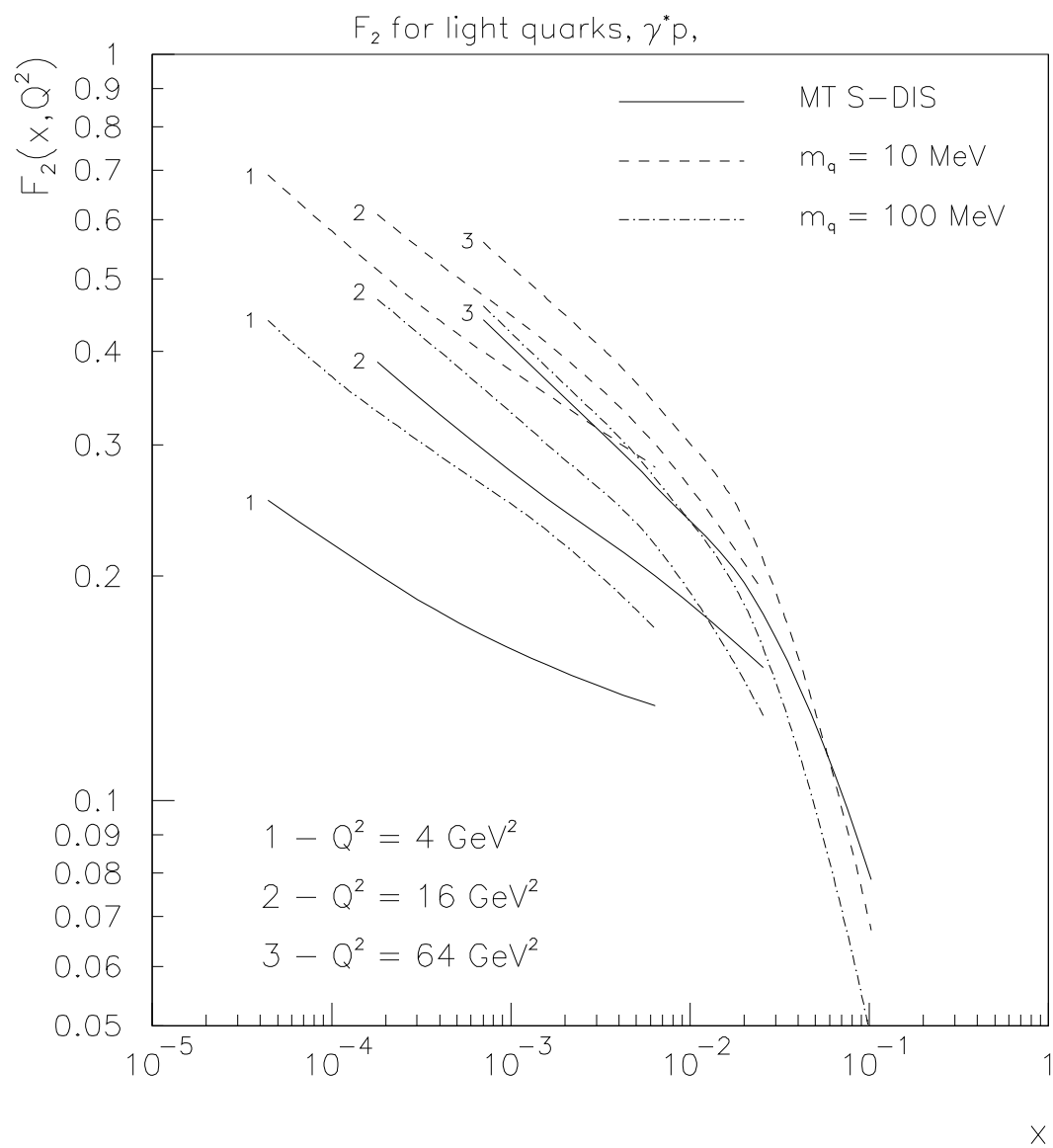


Fig. 2a

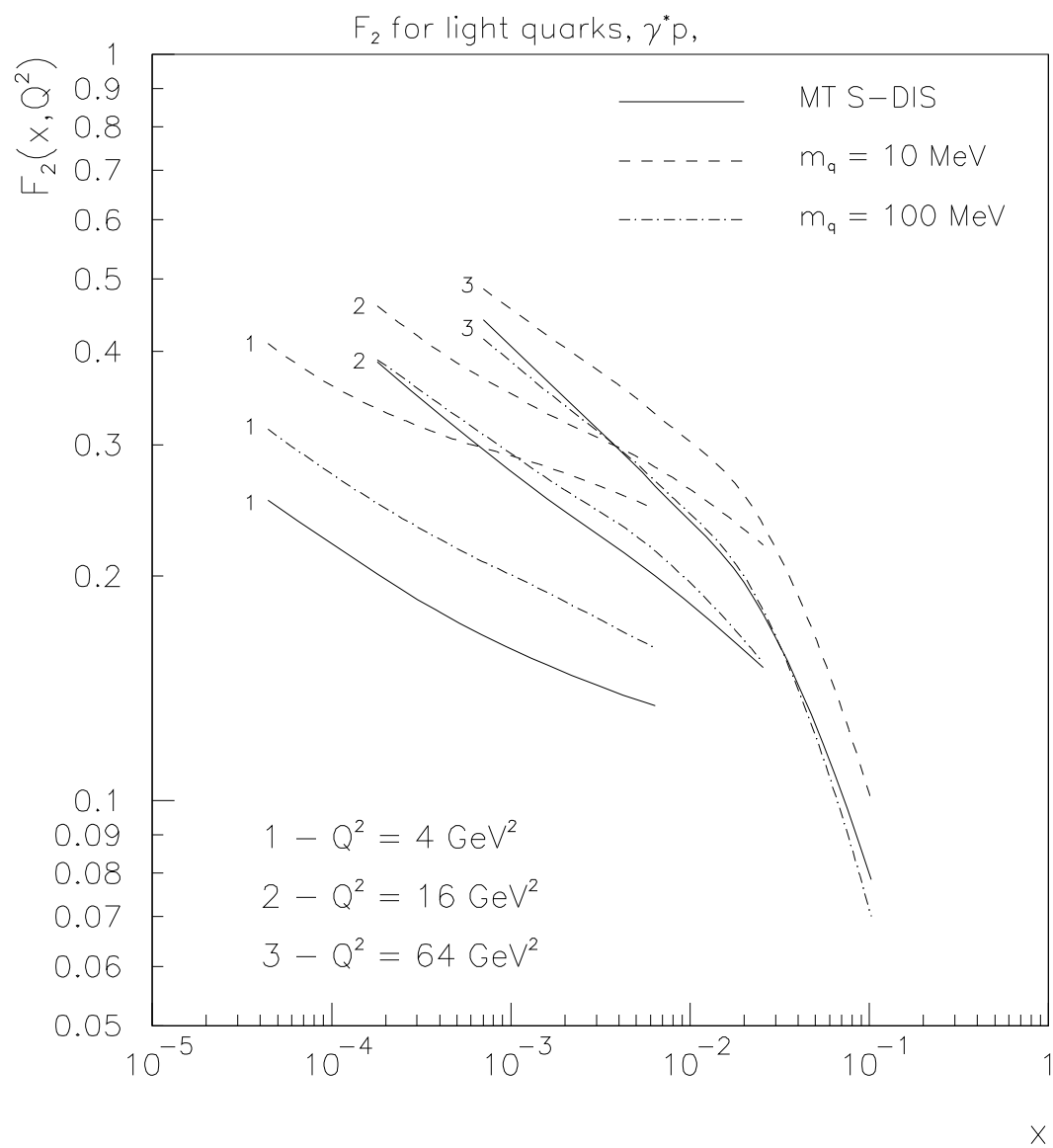


Fig. 2b

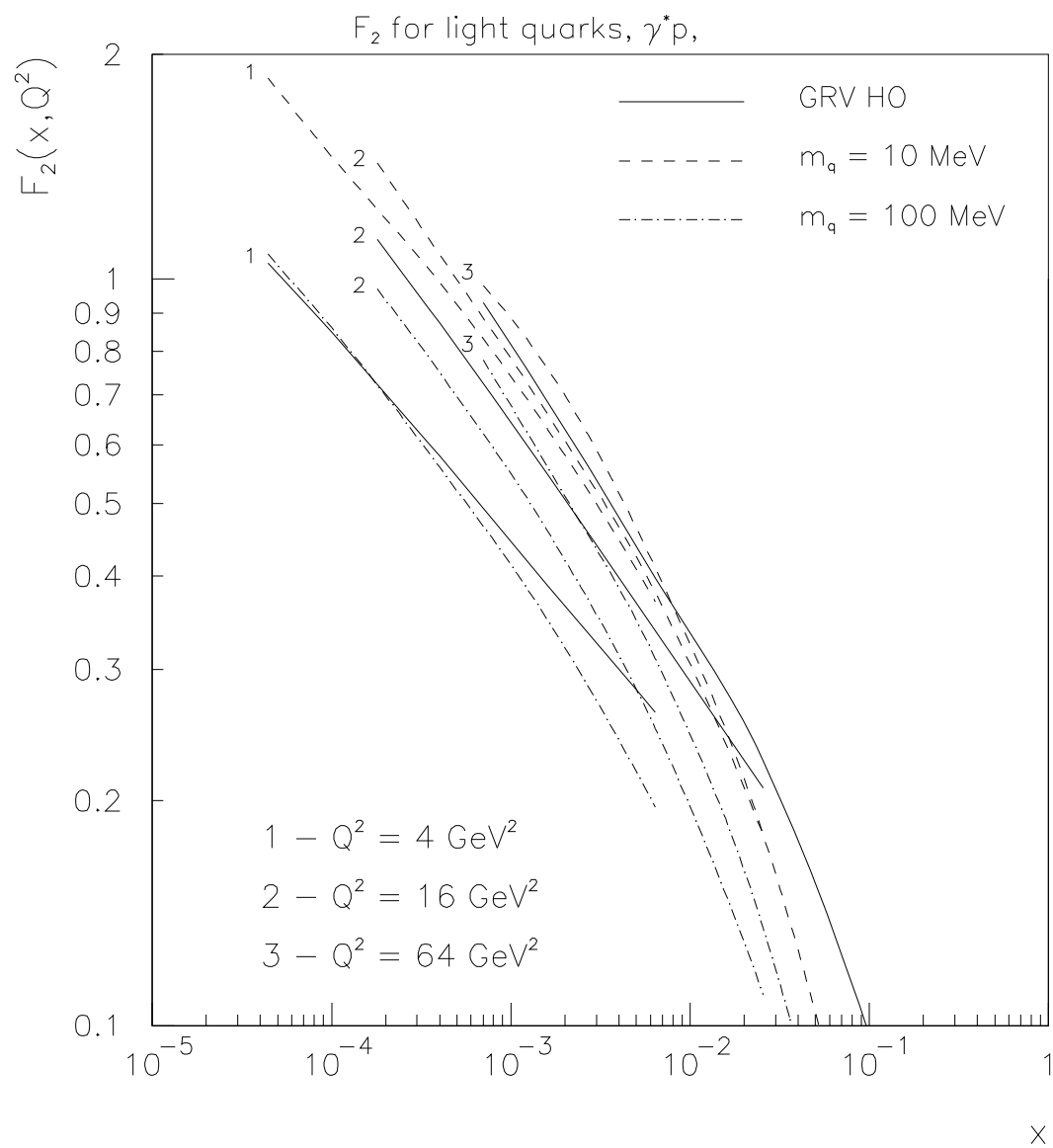


Fig. 3a

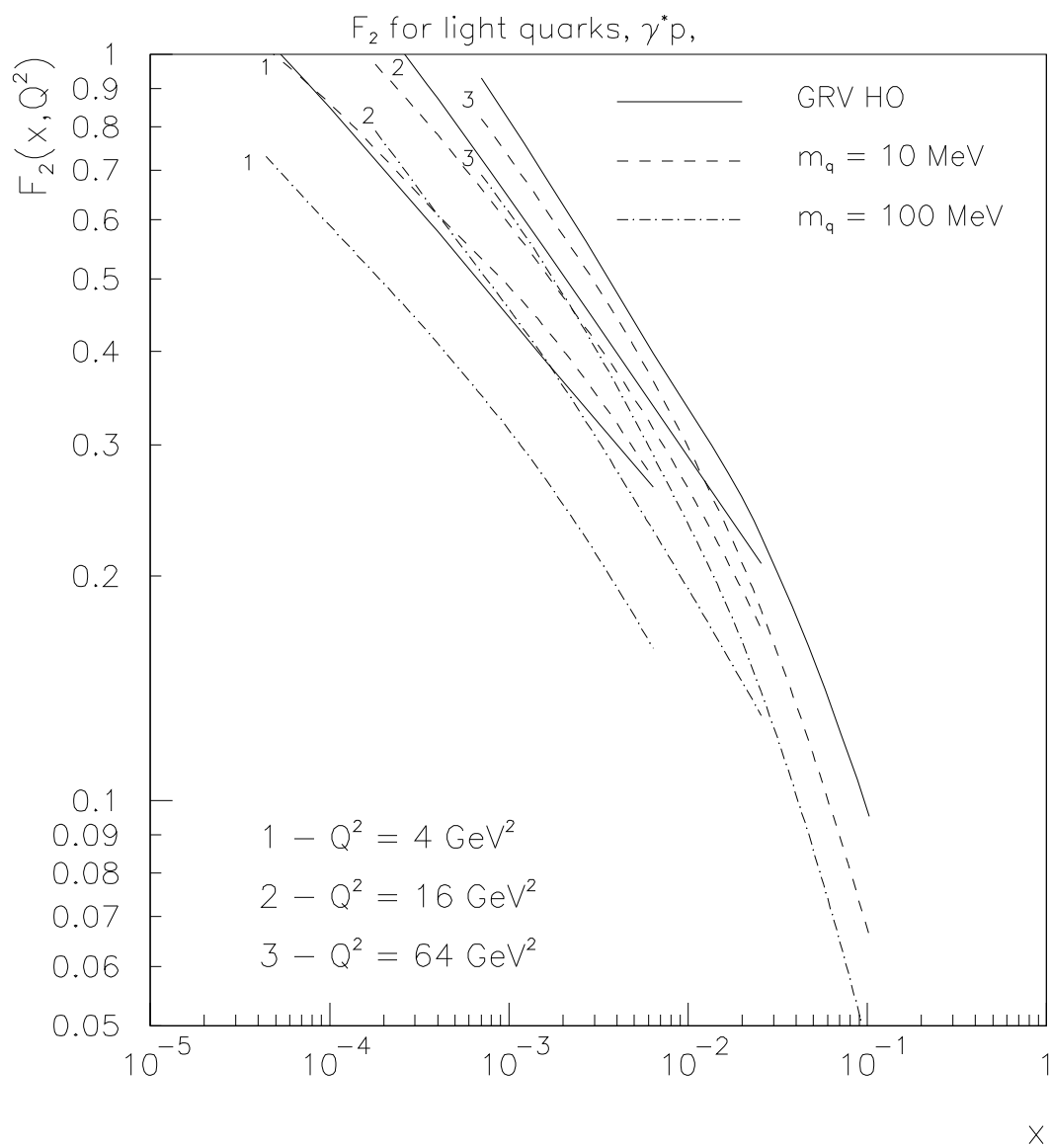


Fig. 3b

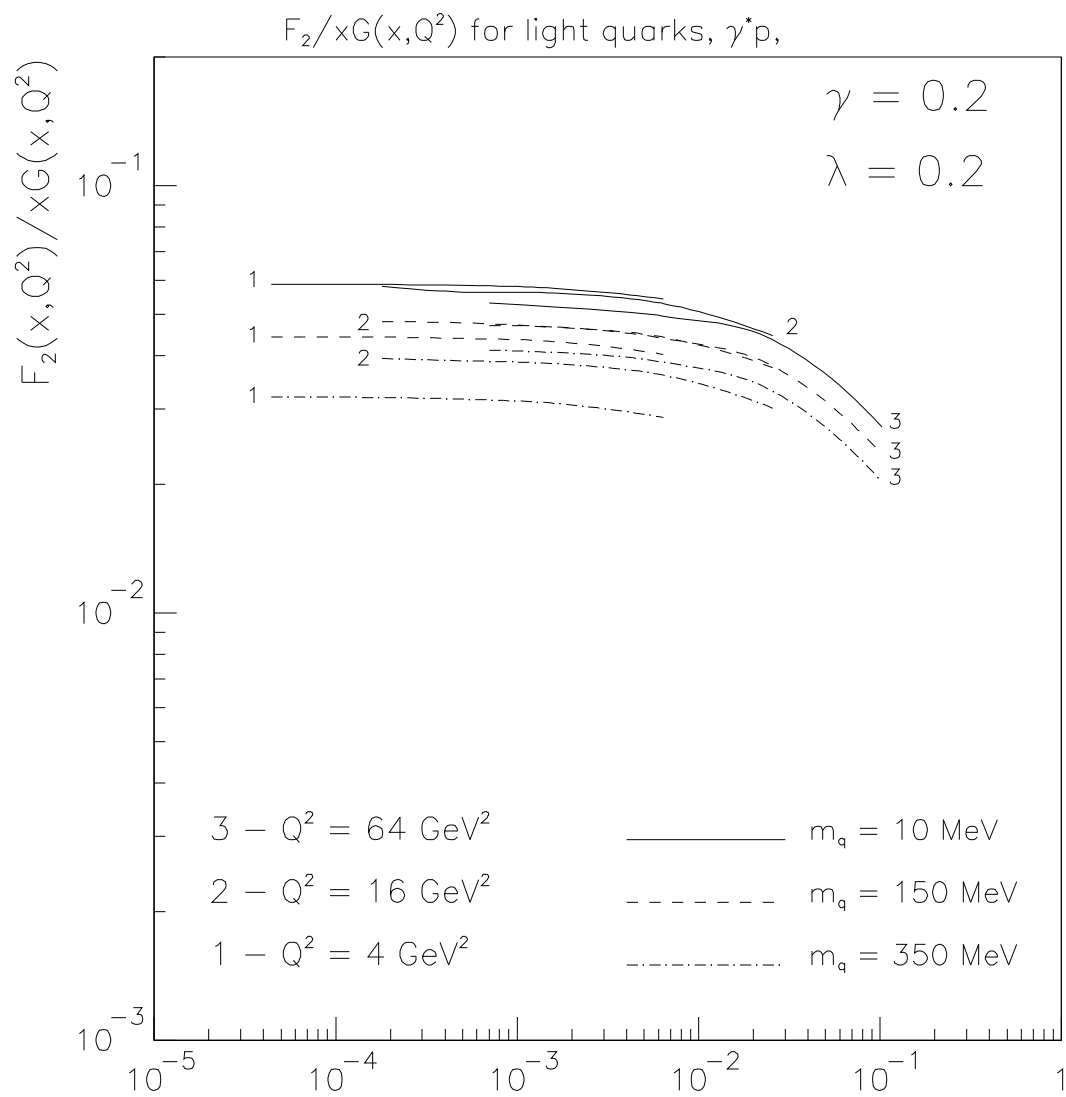


Fig. 4a

x

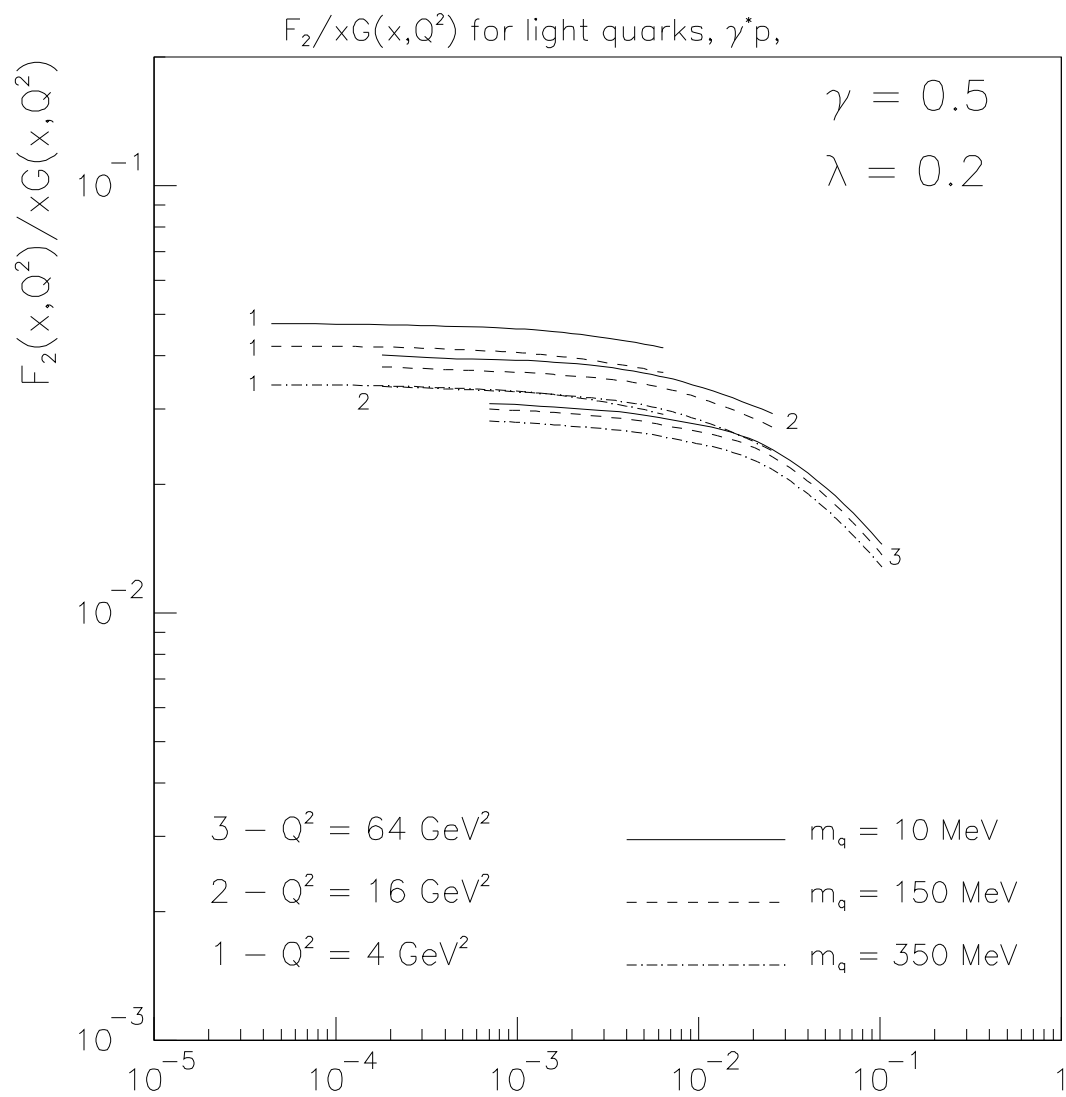
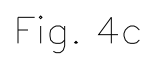


Fig. 4b



X

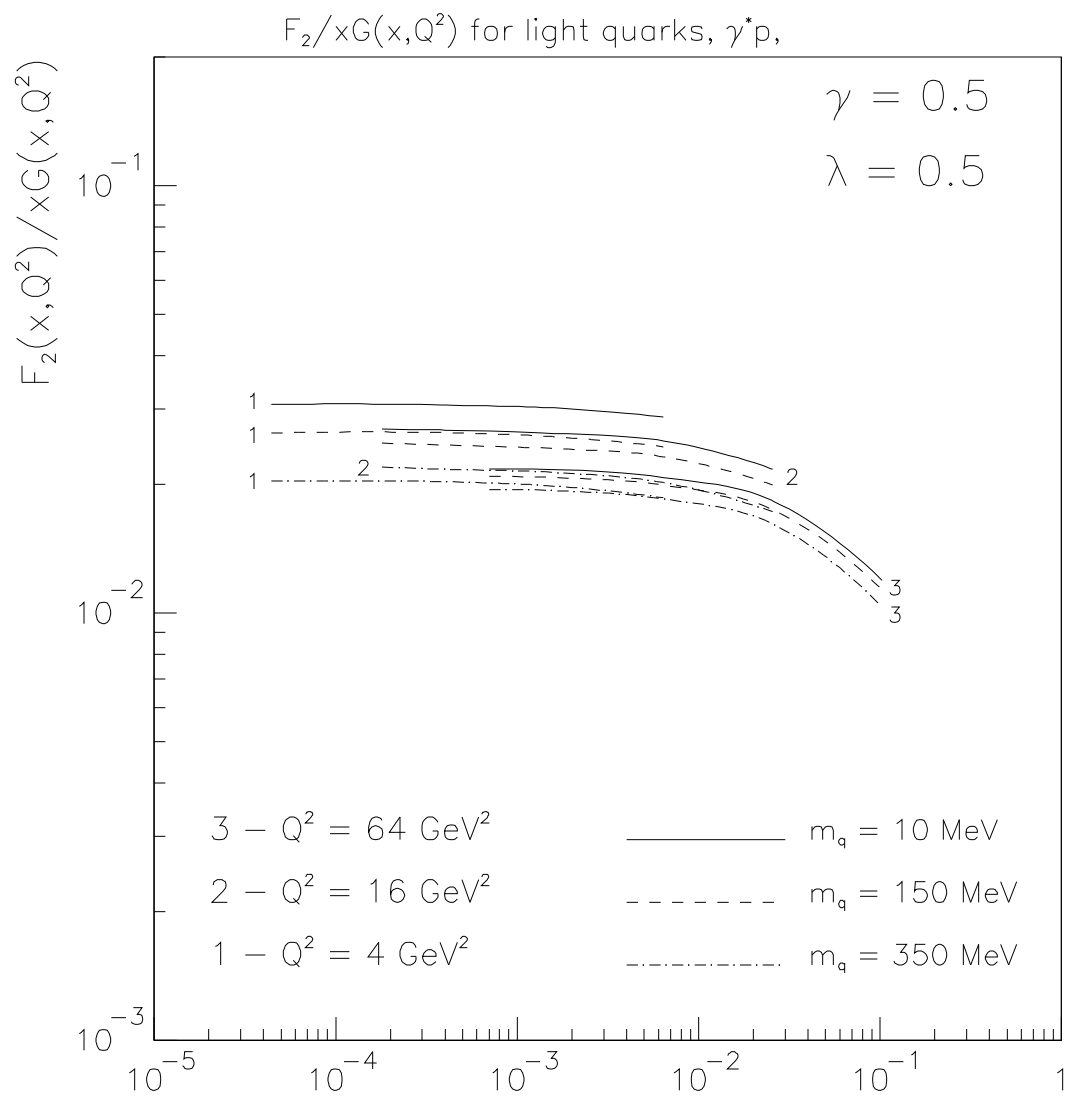


Fig. 4d

x

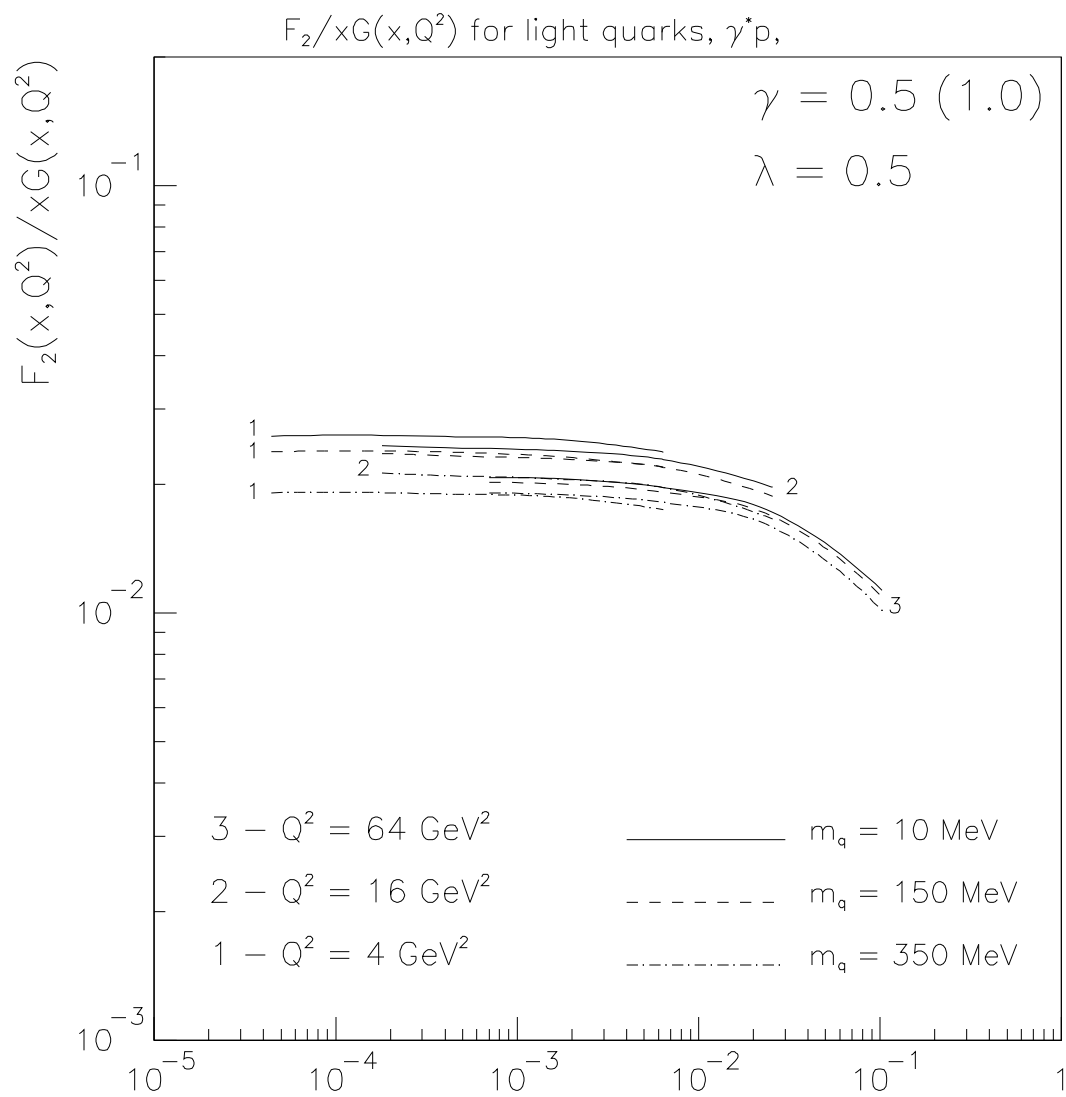


Fig. 5b

x

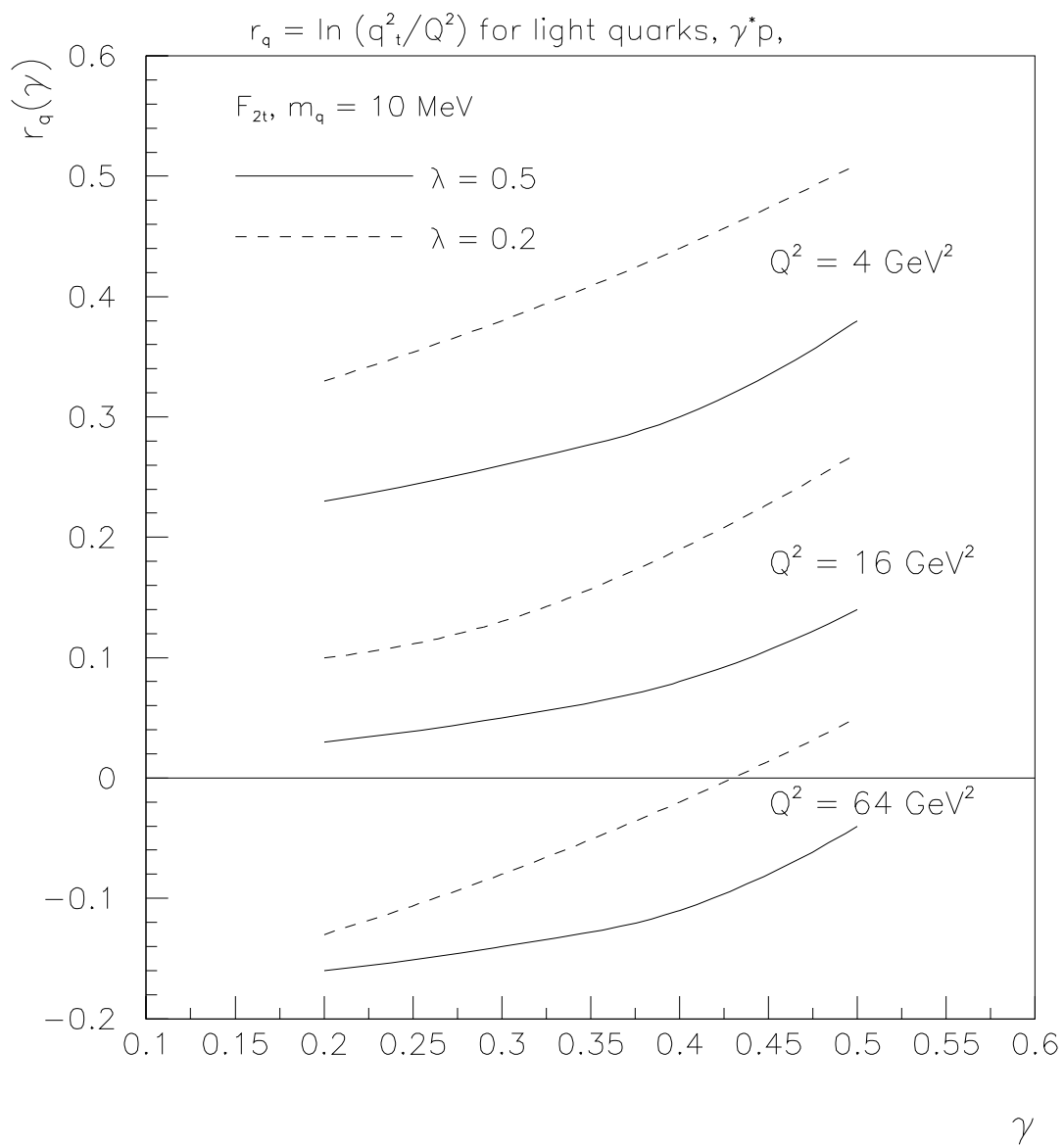


Fig. 6a

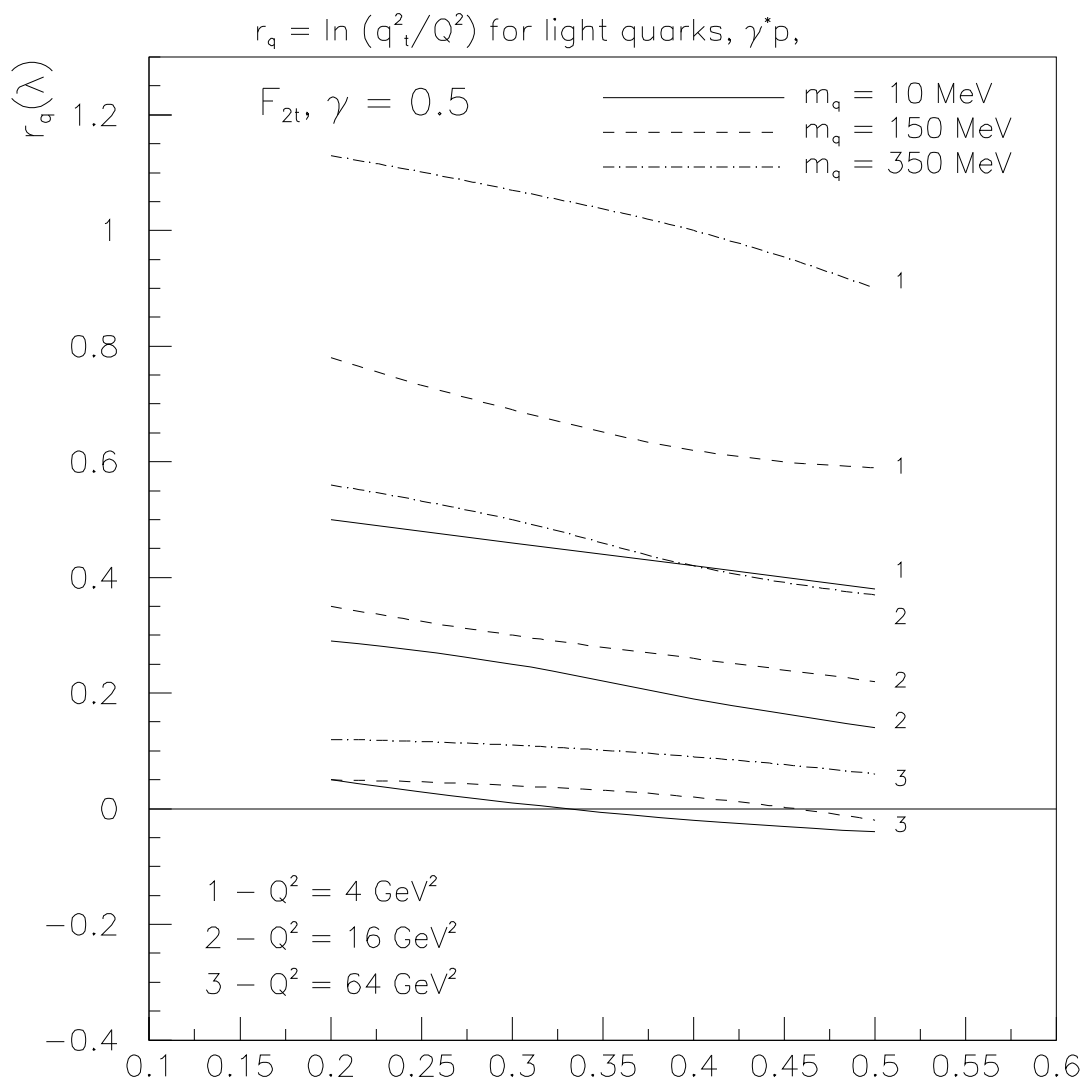


Fig. 6b

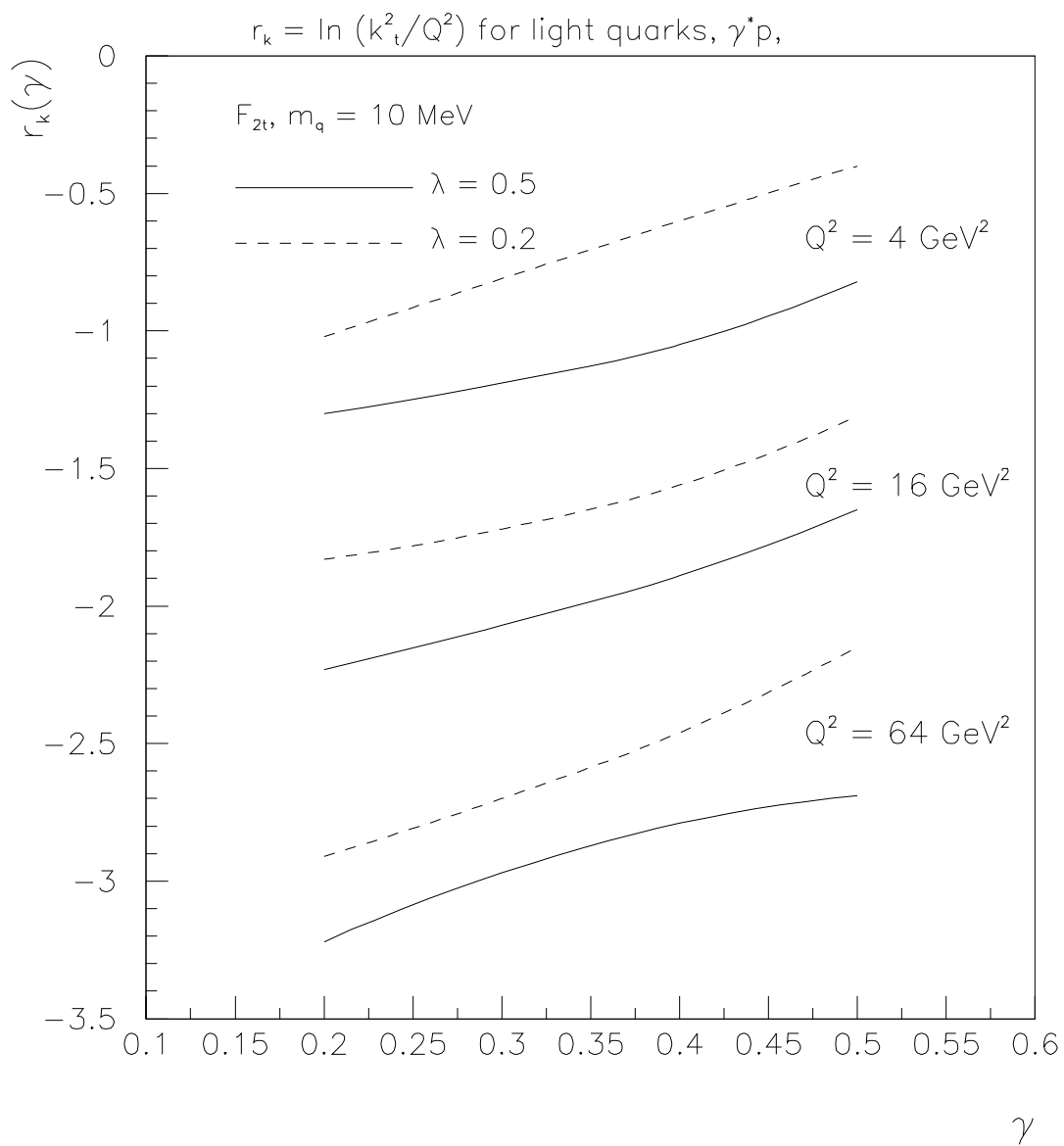


Fig. 7a

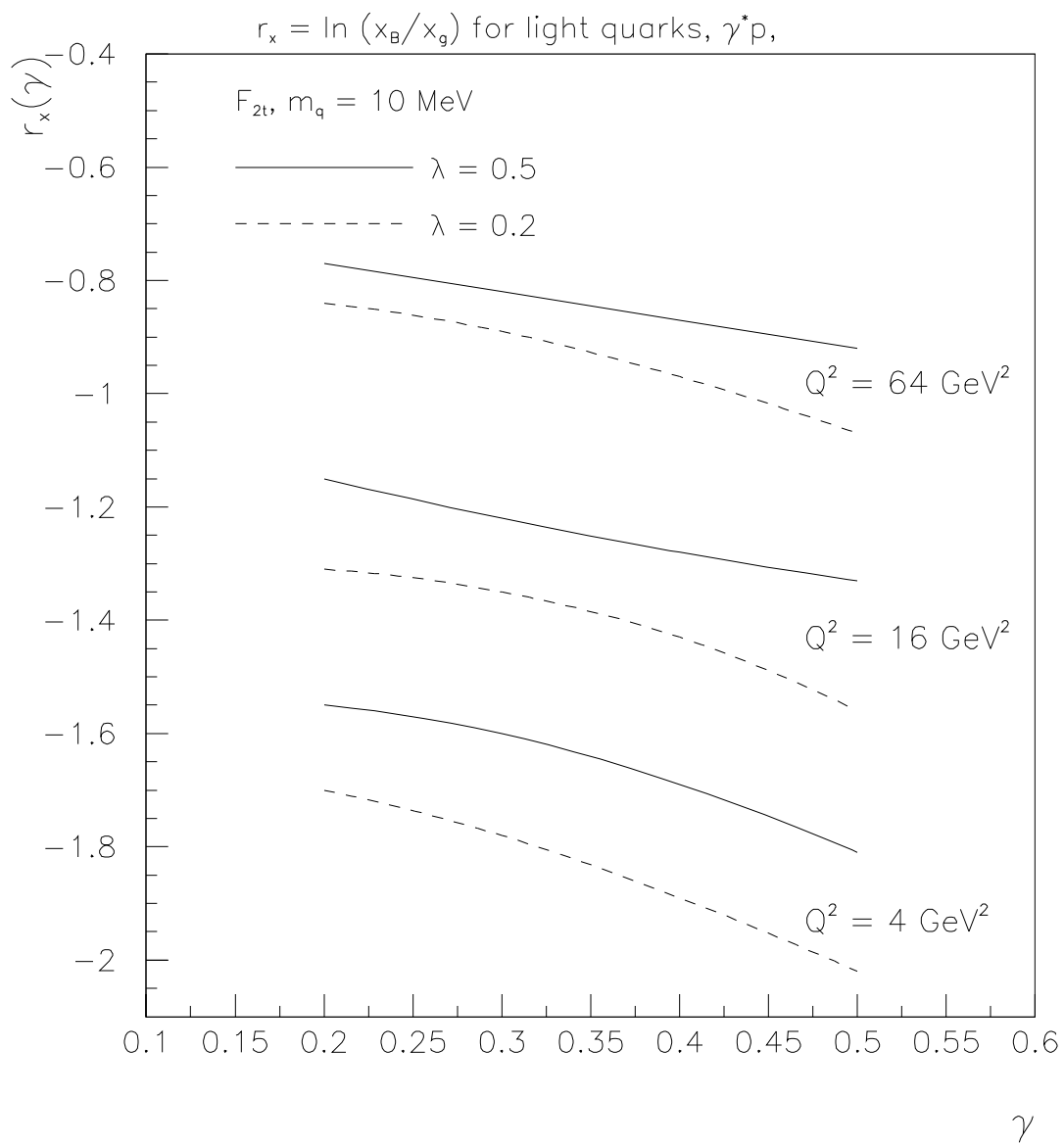


Fig. 8a

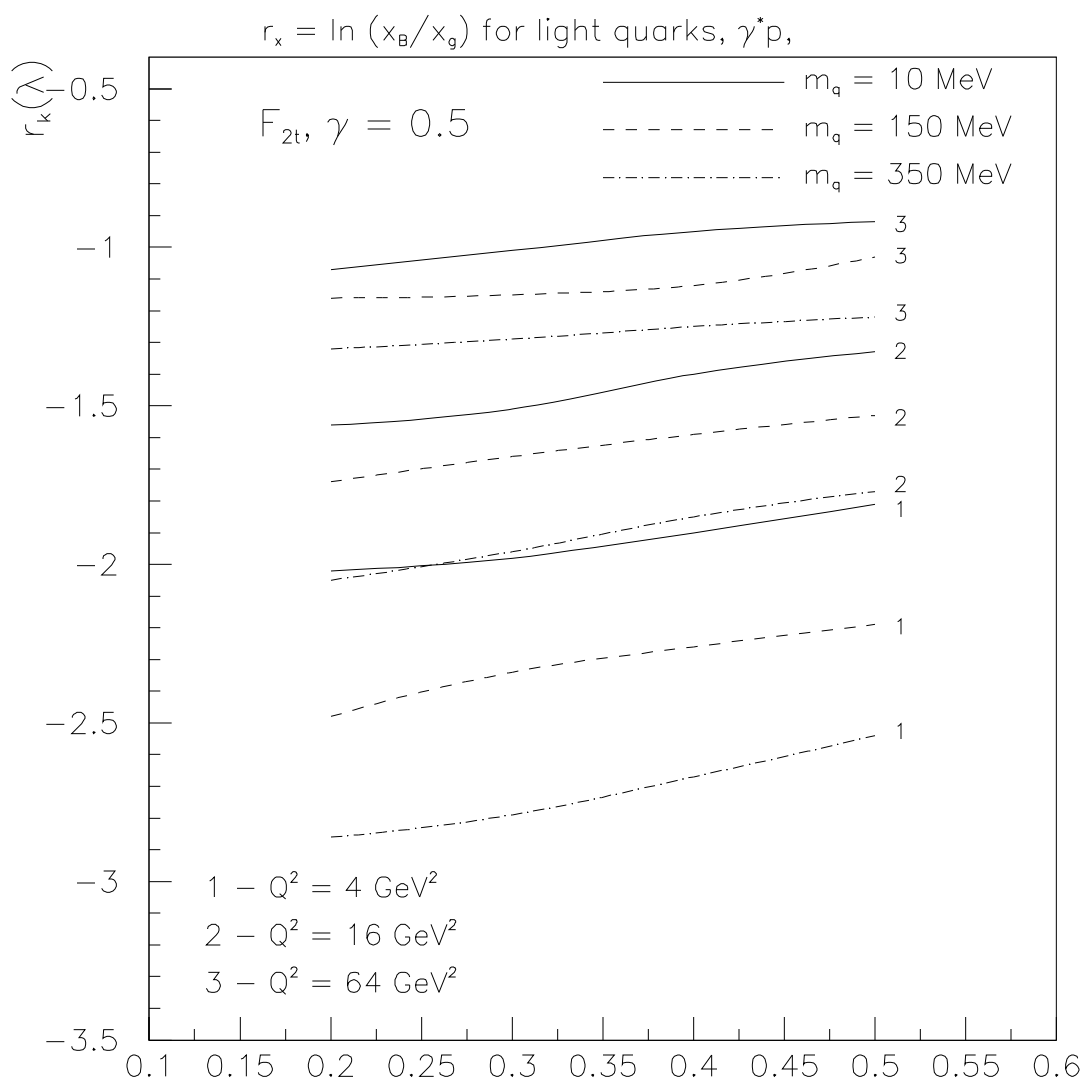


Fig. 8b